euspen's 21st International Conference & Exhibition, Copenhagen, DK, June 2021
www.euspen.eu

Alignment, calibration and data post-processing for on-machine metrology on ultra-precision diamond turning machines

Marco Buhmann[1,2], Thomas Liebrich[1], Raoul Roth[1], Lars Gloor[2], Konrad Wegener[2]

[1]*RhySearch, Buchs SG, Switzerland*
[2]*Institute of Machine Tools and Manufacturing (IWF), ETH Zurich, Switzerland*

marco.buhmann@rhysearch.ch

Abstract
Implementing on-machine measurements on ultra-precision diamond turning machines follows the principle of measuring close to the machining process without reclamping the workpiece and sets up a closed-loop process consisting of machining and measuring. The probe integration into the machine tool inevitably comes along with measurement errors due to alignment, probe system and kinematic imperfections as well as varying scanning conditions. In order to reduce these errors an approach is presented to align the optical axis of an interferometric one-dimensional optical probe parallel to the machine tool spindle axis, necessary to reduce the cosine error caused by misalignment. Furthermore, the approach allows to determine the gain error of the probe system. The machine tool's X-axis straightness deviations in Z-direction are measured and compensated by post-processing of the measurement data. An experimental validation method is presented and yields to a maximum measurement error range of about 45 nm for a measurement of a non-rotational symmetric freeform surface with a diameter of 20 mm.

Keywords: Ultra-precision; In-process measurement; Calibration; Diamond turning

1. Introduction

The achievable accuracy of ultra-precision diamond turning is highly sensitive to various influences like machine tool kinematic deviations or tool offsets. On-machine measurements are an approach to further increase the machining efficiency and follow the principle of measuring close to the machining process. Gao et al. [1] give a broad overview of challenges, requirements and techniques regarding on-machine metrology in precision manufacturing. For the realization of closed-loop machining as well as for measuring machines in scope of quality control like described by Hopper et al. [2], it is important to know the accuracy level of the on-machine measurement data. The measurement error sum comprises probe system errors, machine tool kinematic deviations, effects due to dynamic movements during the measurement, errors related to the scanning parameters in combination with post-processing and filtering as well as thermal displacements. Compared to the work in [3], wherein optical flats are used as a reference surface, the presented approach gives an accuracy estimation for a dynamic freeform measurement using the machine tool axes. The approach is designed to take into account the above mentioned error contributions with the exception that no particular effort is spent to determine or compensate thermal displacements.

For the present work a diamond turning machine of the type LT-Ultra MTC 650 and the interferometric probe system HP-O with an optic head with a numerical aperture of 0.1 is used. The probe is mounted onto an alignment stage, which allows to adjust two angular degrees of freedom as well as one translational in Y-direction of the machine tool coordinate system.

2. Probe axis alignment

2.1 Methodology

Since optical surfaces are commonly machined by face turning, the aim is to align the probe axis parallel to the machine tool's spindle axis as depicted in Figure 1. Since aligning the probe's optical axis by measuring on the probe housing is an indirect method, a direct method is desirable. The measurement situation when measuring against a flat target surface with a tilted probe axis and the corresponding geometrical correlations are shown in Figure 2. The flat target is assumed to be perpendicular to the Z-axis, since the squareness error between the X-axis and the spindle axis is usually less than 100 nm over 50 mm of X-travel. A tilt of the probe axis by any combination of the tilt angles α and β results in an extended measured probe distance $z_{P,t}$, what is given by equation (1). By moving the Z-axis according to a sine function and measuring the movement by the probe system measuring against the flat target, a certain probe measurement range of length $z_{P,t}$ is tested. The Z-positions z_M measured by the machine tool's internal glass scale of the Z-axis are recorded as well and represent the nominal values. By using equation (2), the differences Δz_P between the probe distances and the recorded Z-positions z_M can be derived. Plotting Δz_P as function of the nominal Z-positions z_M allows to define the angle γ by applying a linear least squares fit to the noisy probe data. Figure 5 depicts the definition of the angle γ.

$$z_{P,t} = \frac{z_P}{\cos\beta\,\cos\alpha} \quad (1)$$

$$\Delta z_P = z_{P,t} - z_M \quad (2)$$

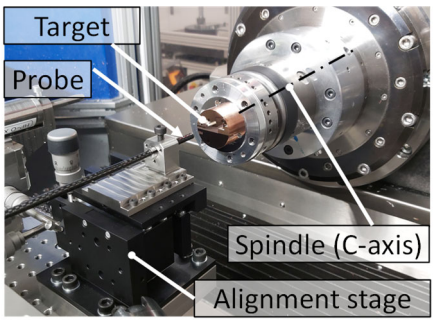

Figure 1. Measurement situation used for the present work.

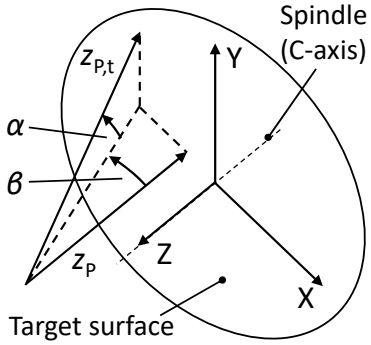

Figure 2. Measurement situation for probe axis alignment. Machine tool coordinate system (X-Y-Z) and geometrical correlations of the tilted probe axis. Nominal probe distance z_P; probe distance $z_{P,t}$ as a result of a tilt by the tilt angles α and β (indicated are the positive directions of α and β).

By supposing that the probe system itself has an unknown gain error, the angle γ comprises the error sum caused by a probe axis tilt and the gain error. Due to the fact that a probe axis tilt can only lead to a positive change of the angle γ, the probe axis perpendicularity to the target surface should be able to be found by searching the minimum angle γ. This can be done by determining the values of γ for various probe tilt angles α and β by adjusting the angles using the alignment stage.

It should be noted that the method assumes a linear probe behavior, i.e. the probe system's non-linear errors should be sufficiently small to be neglected. Otherwise the non-linearities additionally affect the determination of the angle γ, what prevents to be able to derive the probe axis tilt out of it. Therefore, the probe's linearity is previously investigated by testing various measurement ranges of the probe. Figure 3 shows the differences Δz_P for a tested probe range of 70 µm. As can be seen, the used probe starts to show non-linear errors at increasing absolute nominal values, while a linear behavior can be supposed within 20 µm symmetrically arranged around the nominal value of zero. It is noted, that the probe value of zero is calibrated to correspond to the focus point of the probe. An optimum measurement range is always symmetrically arranged around the probe's focus point.

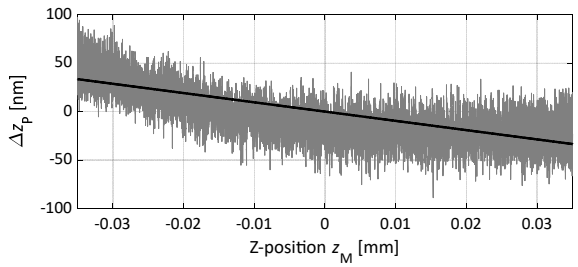

Figure 3. Probe error differences Δz_P for a tested measurement range of 70 µm symmetrically arranged around the probe's focus point.

2.2 Results

To take the observed probe behavior into account, the probe range to be tested is set to be 20 µm and realized by moving the Z-axis according to a sine function with an amplitude of 10 µm. The tilt angles are both adjusted in a range of - 2° to + 2° in steps of 0.5° using the alignment stage. The zero positions of α and β are preliminary set by measuring along the probe housing using a dial gauge. As target surface a plane perpendicular to the Z-axis is machined in oxygen-free copper. The method is first applied varying only the angle β. Figure 4 shows the resuling values of γ as function of the adjusted β-values. To test the repeatability, each β-value is measured twice. Before applying the method for the minimum search over α, the probe axis is adjusted and set to β = - 1°. By varying the angle α over the same range the minium slope angle is found at α = - 0.5°.

The residual probe error for the set values of the tilt angles is depicted in Figure 5 and is considered as the gain error of the probe system. At a probe value of + 10 µm respectively - 10 µm the absolute error is about 35 nm.

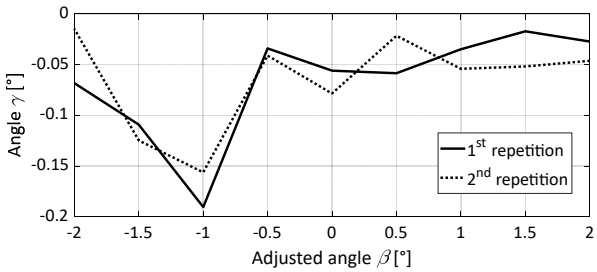

Figure 4. Slope angles γ as function of the adjusted tilt angles β.

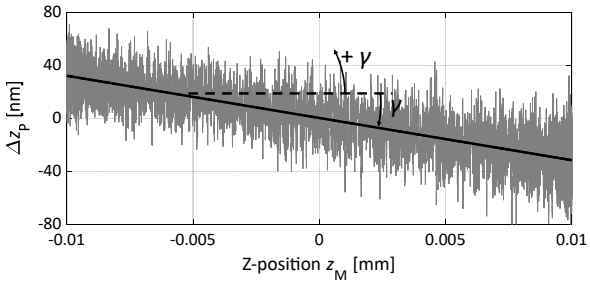

Figure 5. Residual probe error Δz_P after angular alignment of the probe axis as function of the nominal values given by the Z-positions z_M and definition of the angle γ.

2.3 Discussion

Besides the observeable differences between the repetitions in Figure 4, the derived γ-values does not follow the theoretical geometrical correlations given in Figure 2. According to them, the angle γ should further increase between the β-values of - 0.5° and - 2°, but these stay on a rather constant level instead. So, the received probe behavior and γ-values do not exactly agree with the expected behavior, but show clear minimum values at β = - 1° and α = - 0.5°. Table 1 summarizes the calculated values of Δz_P for tilt angles β between 1° and 5° and different values of z_P. It can be seen, that the differences for z_P = 20 µm (as tested in the previous section) are around 12 nm for the tested maximum tilt angle of 2°. Due to the fact that the smallest moveable step of the Z-axis of the employed diamond turning machine with 10 nm is about the same scale, the results of the probe axis alignment method can not be assigned to the changes of the probe axis tilt angles with sufficient certainty.

Nevertheless, the method serves to characterize the non-linear and linear errors of the probe system, of which the latter are treated as the gain error. Additionally, it turned out that the probe error changes with small changes of the tilt angle,

what is shown by the large difference of the angle γ between the values β = - 1° and β = - 0.5°.

With the assumption of an angular probe axis tilt of 1°, the error contribution of the tilt is about one order smaller (3 nm according to Table 1) compared to the maximum error values shown in Figure 5. Since the used probe measurement range when measuring form errors of diamond turned surfaces mostly lies below 5 µm, the error resulting out of an angular misalignment of 1° can be neglected. However, this is not the case for the residual gain error depicted in Figure 5. Even when measuring at a nominal value of 2.5 µm an error of 8.75 nm occurs as a result of the determined gain error.

A resulting lateral shift of the measuring point for a measurement range of 5 µm due to an angular tilt of 1° can be estimated by using the sine function to be 87 nm, what is more than 100 times smaller than the light spot diameter at the focus point. The effect of an lateral shift on the measured distance in Z-direction depends on the slope of the measured surface and can be estimated using trigonometry to be < 5 nm for slope angles of up to 3°.

Table 1. Calculated values of Δz_P in function of various tilt angles β and values z_P.

β [°]	Δz_P [nm] (z_P = 2 µm)	Δz_P [nm] (z_P = 20 µm)	Δz_P [nm] (z_P = 30 µm)
1	0.3	3	4.6
2	1.2	12.2	18.3
3	2.7	27.4	41.2
4	4.9	48.8	73.3
5	7.6	76.4	114.6

3. Measurement of X-axis straightness

Besides the squareness error between the X-axis and spindle axis, X-axis straightness deviations in Z-direction directly affect the measurement results of on-machine probe-scan systems. To compensate these deviations, the X-axis straightness is determined utilizing the setup depicted in Figure 6. It cosists of an optical flat mounted directly to the Z-axis slide to eliminate vibrations and thermal displacements of the spindle axis. The use of an optical flat having a peak-to-valley flatness error < 3 nm over a diameter of 30 mm allows to measure the straightness deviations in function of the probe's X-position without a reversal measurement by performing a linear scan along the flat's diameter. For that, the flat is aligned nearly parallel to the X-axis in order to keep the probe distances over 30 mm of X-travel within 3 µm. The residual non-paralellism to the X-axis is corrected afterwards by applying a linear regression. To determine the probe's position with regard to the spindle axis, the procedure presented in [4] is used.

Figure 7 depicts the deviations of ten repeated linear scans and their mean. The smallest moveable step of the Z-axis (10 nm) and temperature deviations are assumed to be the main reasons for the differences between the repetitions, which lie within 20 nm. Besides these differences, the general behavior of the repetitions along the measured X-distance agrees, what allows to represent the X-axis straightness by their mean.

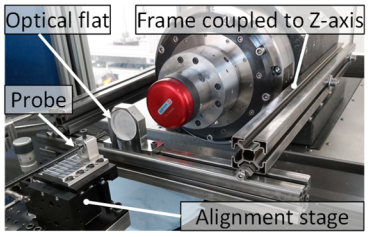

Figure 6. Setup to measure the X-axis straightness deviations.

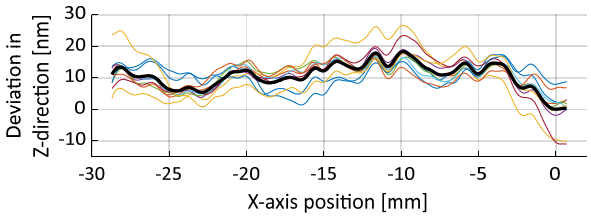

Figure 7. X-axis straightness: Deviations in Z-direction. Ten repeated linear scans (coloured); arithmetic mean (black).

4. Measurement accuracy estimation

4.1 Methodology

An experimental validation for the on-machine measurement accuracy turns out difficult because positioning inaccuracies when mounting a reference artefact onto the C-axis always add errors, what is also mentioned by Li et al. [3]. An alternative approach is to machine a flat target surface and to simulate a form error by generating a controlled relative displacement of the probe by a path programmed on the machine tool. As long as machining and measuring take place on the same side of the machine tool's X-axis, the approach is not affected by a kinematic squareness error between the X-axis and the spindle axis (C-axis). Therefore, the approach allows to prove the accuracy of the measurement system consisting of the machine tool and the integrated probe system without being affected by the mispositioning of an artefact as well as to test various error forms and scanning parameters. However, an additional measurement uncertainty due to unknown probe offsets has to be considered since the present approach is not affected by possible probe offsets.

To take into account the form error of the flat as a result of the machining process, a radial scan is performed and the result is used to subsequently compensate the areal measurement data of the proposed approach. Figure 8 depicts the measured form error as function of the radius respectively the X-position of the probe. The values are set to zero at the X-position of zero and lie in the same range as the measured straightness deviations (see Figure 7). Although the machining process uses another area of the machine tool's X-axis, the measured form error is supposed to be mainly caused by the X-axis straightness deviations in Z-direction.

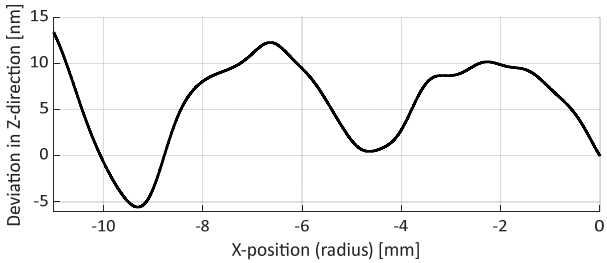

Figure 8. Measured form error in Z-direction of the machined flat that serves as measurement target.

4.2 Results

Figure 9 describes the approach and shows the tested form error function according to equation (3), in which x, y and z are the coordinates of the scanning trajectory programmed to the machine tool. The resulting differences between the distances measured by the probe and the Z-axis positions recorded during the measurement give an estimation of the system's measurement accuracy. Figure 10 shows the differences without the compensation of the measured X-axis straightness deviations in XY-view and XZ-view and Figure 11 the same with the X-axis straightness compensation applied. A two-dimensional second order robust Gaussian regression filter

is applied along cylinder coordinates of the raw data. The data is recorded by a spiral trajectory with 30 µm spacing between the rotations and a C-axis speed of 19 rpm. The X-axis straightness compensation improves the error in the center area within a diameter of 6 mm but also increases the overall error range by 5 nm, what can be related to the uncertainty of the straightness measurement represented by the repetitions shown in Figure 7. Figure 12 additionally shows a sectional view at Y = 0 of Figure ***11*** (a). Since this sectional view does not agree with the shape of the target's form error (see Figure 8) and mean X-axis straightness deviations (see Figure 7) and since these errors are already compensated, thermal displacements in the sensitive Z-direction during the measurement, for example of the spindle rotor unit or the probe support, are supposed to be a possible reason for the residual measurement error, which mainly depends on the radial coordinate of the measurement.

$$z(x,y) = 0.001 \cos\left(x\frac{\pi}{8}\right)\cos\left(y\frac{\pi}{8}\right) \qquad (3)$$

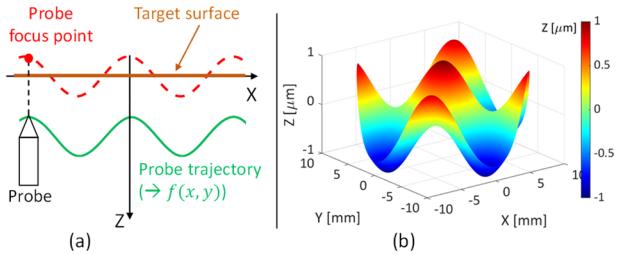

Figure 9. Accuracy estimation approach (a) and tested form error (b).

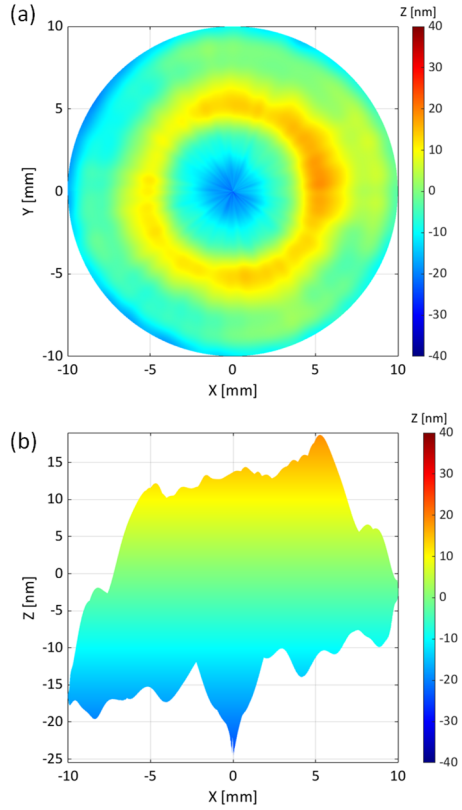

Figure 10. Without straightness compensation: Differences between probe distances and recorded machine tool Z-positions. XY-view (a) and XZ-view seen in direction of the positive Y-axis (b).

5. Summary

The presented work gives an accuracy estimation for optical on-machine surface form measurements. For a freeform measurement over a diameter of 20 mm with three machine tool axes simultaneously moving a maximum error range of around 45 nm is specified. The proposed method for the probe axis alignment helps to estimate the effect of a probe axis tilt and determines the gain error of the probe system so that it can be corrected by post-processing of the measurement data. Using a high accurate optical flat allows to measure the X-axis straightness deviations in Z-direction without a reversal measurement. The effect of their compensation is shown. Further investigations will cover dynamic and thermal influences as well as influences of different filtering methods and the potential of closed-loop freeform machining.

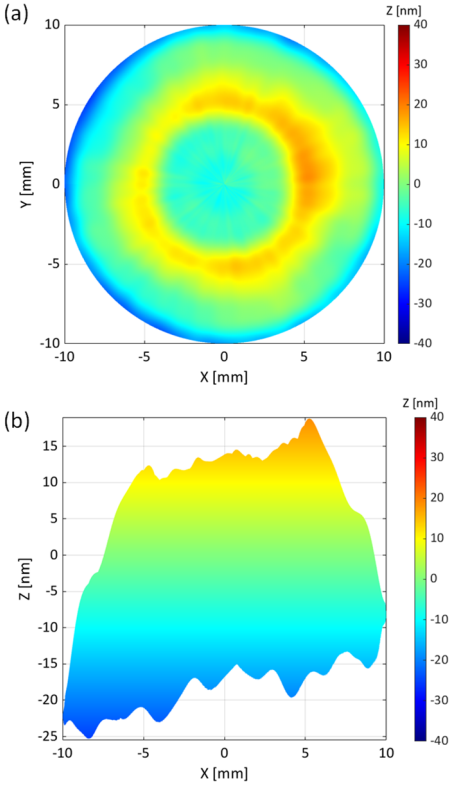

Figure 11. With straightness compensation: Differences between probe distances and recorded machine tool Z-positions. XY-view (a) and XZ-view seen in direction of the positive Y-axis (b).

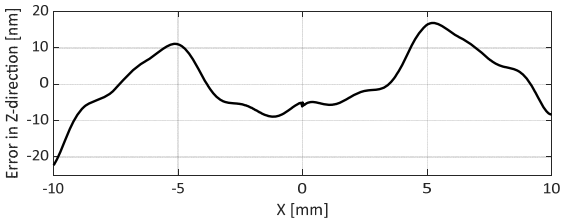

Figure 12. With straightness compensation: Differences between probe distances and recorded machine tool Z-positions; sectional view at Y = 0.

References

[1] Gao W., Haitjema H., Fang F.Z., Leach R.K., Cheung C.F., Savio E. and Linares J.M., 2019, On-machine and in-process surface metrology for precision manufacturing, *CIRP Ann.*, vol. **68**, no. 2, pp. 843–866.

[2] Hopper L., Noste T., Miller J. and Evans C., 2020, Error sources, compensation, and probe path optimization for on-machine metrology of freeform optics, *Proc. of SPIE **11487**, Optical Manufacturing and Testing XIII*, 1148709.

[3] Li D., Tong Z., Jiang X., Blunt L. and Gao F., 2018, Calibration of an interferometric on-machine probing system on an ultra-precision turning machine, *Measurement*, vol. **118**, pp. 96–104.

[4] Buhmann M., Roth R., Liebrich T., Frick K., Carelli E. and Marxer M., 2020, New positioning procedure for optical probes integrated on ultra-precision diamond turning machines, *CIRP Ann.*, vol. **69**, no. **1**, pp. 473–476.